Journal of Infection 92 (2026) 106696

Contents lists available at ScienceDirect

Journal of Infection

journal homepage: www.elsevier.com/locate/jinf

Viruses and Viral Diseases

Comparative cross-species transcriptomics during RSV infection identifies targets to treat RSV disease

Ziyin Wang [a,1], Claire Dunican [a,b], Pete Dayananda [a], Suhaylah Ingar [a], Myrsini Kaforou [a,b], Christopher Chiu [a], John S. Tregoning [a,*]

[a] Department of Infectious Disease, Imperial College London, SW7 2AZ, UK
[b] Centre for Paediatrics and Child Health, Imperial College London, UK

ARTICLE INFO

Article history:
Accepted 28 January 2026
Available online 31 January 2026

Keywords:
RSV
Transcriptome
IL-17
Mouse
Infection
Lung
Human challenge

SUMMARY

Respiratory syncytial virus (RSV) remains a health threat to young children worldwide. The host immune response plays a key role in disease following infection. Infection models advance our understanding of respiratory viruses, but individual models have gaps, which overlapping complementary systems can fill. We compared disease signatures in mice, adults and children; combining transcriptomic data collected from blood, nasal mucosa and lung biopsy following RSV infection. We identified both shared and species-specific pathways triggered by RSV. While systemic responses in children's blood were more similar to those in RSV-challenged adults, mucosal responses during primary infection in mice more closely resembled those in children. We identified an association between IL-17 pathways and RSV pathogenesis and with over-expression of the downstream effectors S100A8 and S100A9. Inhibiting these with the anti-inflammatory drug Paquinimod reduced disease. Here we demonstrate that integrating mouse and human transcriptomic data can identify novel targets to treat RSV disease.
© 2026 The Author(s). Published by Elsevier Ltd on behalf of British Infection Association. This is an open access article under the CC BY license (http://creativecommons.org/licenses/by/4.0/).

Introduction

Respiratory syncytial virus (RSV) is the primary cause of severe lower respiratory tract infection (LRTI) among infants and young children globally. Worldwide, RSV is responsible for 33.1 million cases in children per year, with 3.2 million hospital admissions and 59,600 in-hospital deaths.[1] Children under six months of age are at a higher risk of hospitalisation and fatal outcomes, accounting for 50% of total hospitalised LRTI cases in high-income countries.[2] Whilst the newly licensed vaccines and antibodies will reduce the burden of infection, limitations in availability and uptake mean that there will still be a high burden of disease, particularly in low-income countries. Understanding RSV disease in infants and young children is an indispensable step in the search for novel therapies. Systems-scale data collection and network analysis facilitate unbiased mechanistic insights into disease,[3] which in turn can help identify drug targets.

Although natural RSV infection in children is the disease of interest, it is very difficult to study directly in this population. This is due to the extreme difficulty of collecting lower respiratory tract samples as symptoms worsen, the unknown kinetics of infection (when the child was first infected) and the contribution of other confounders such as co-infections. Building on the aphorism that all models are wrong, but some are useful,[4] triangulating different datasets can help fill in the gaps of understanding. Here, we compare mouse and human challenge models as they share the strengths of known kinetics, baseline immune status, challenge dose and strain. Whilst human adults are the same species, challenge models mostly use healthy, young volunteers who are immunologically mature and highly RSV-experienced. As these volunteers typically experience mild-to-moderate disease, they may not reflect the situation in RSV-naïve children as the induced disease and observed host responses will inevitably differ to those in infant bronchiolitis.[5] Meanwhile, interspecies differences in physiology, behaviour, viral tropism and genetics may limit aspects of the translatability of mice studies. For example, severe RSV infection in human infants results in a predominantly neutrophil infiltrate, whereas in mice, these leucocytes do not dominate and comprise no more than 20% of the airway infiltrate.[6] But mouse models allow access to all tissues, the ability to perform biological repeats in genetically identical individuals, tools to manipulate the response to investigate mechanism and the possibility to alter the degree of previous antigen exposure.[7] Therefore, combining these different approaches can compensate for limitations.

* Corresponding author.
E-mail address: john.tregoning@imperial.ac.uk (J.S. Tregoning).
[1] Present address: La Jolla Institute for Immunology, CA, USA.

https://doi.org/10.1016/j.jinf.2026.106696
0163-4453/© 2026 The Author(s). Published by Elsevier Ltd on behalf of British Infection Association. This is an open access article under the CC BY license (http://creativecommons.org/licenses/by/4.0/).

We and other groups have observed a key role for excess lung inflammation in RSV disease.[8] Clinical interventions with steroids and anti-IL-6 in patients with severe COVID-19 demonstrated that immunomodulation can reduce severe respiratory disease. Studies such as REMAP-CAP demonstrated opportunities for repurposing orphan anti-inflammatory drugs to treat respiratory disease.[9] Understanding which inflammatory mediators play a role in RSV disease will help identify novel treatment options; transcriptomics can help down-select possible interventions. One aspect adding to the complexity of understanding disease mechanism is that sampling different tissue types can provide different levels of information. High expression of the proinflammatory cytokines TNF, CXCL8 and IFNγ in the bronchoalveolar lavage (lower airway) is positively associated with RSV bronchiolitis severity, whilst in contrast low serum levels of the same three mediators (TNF, CXCL8 and IFNγ) have been associated with severe disease.[10] Thus, approaches comparing different compartments are needed to more clearly determine key drivers of disease.

By describing the transcriptomic outcomes of RSV infection in the blood, lung and nasal mucosa across children, adult and mouse models, we aimed to construct an unbiased approach to investigate how accurately mouse and adult deliberate challenge models reflect natural RSV infection in young children. We observed that in blood, the host response in adults challenged with RSV resembled that of children infected with RSV. However, the mouse model correlated better with children for upper airway responses and therefore can be a useful tool to identify mechanisms of bronchiolitis. Further exploration of the shared pathways between mouse and infants confirmed an association between IL-17 pathways and RSV pathogenesis. We identified a novel role for S100, a functional effector downstream of IL-17; blocking this with the immunomodulatory drug Paquinimod reduced disease following infection. Therefore, cross systems comparisons can provide a platform to identify potential targets for new therapeutics.

Results

Blood transcriptomes following RSV infection show limited similarities between systems

The aim of the study was to identify transcriptomic patterns across human and mouse models of RSV disease and compare them to natural RSV infection in children, as one of the major high-risk groups, to improve our understanding of the mechanism of disease. We started by looking at responses in blood, as a more accessible compartment. For the child dataset, blood samples were collected on day of hospitalisation from children with severe RSV and compared to controls. We only used data from female children, to reduce one source of variability. Severe RSV positive children were between 0 and 79 months old and the control children were aged between 0 to 208 months old. For the adult dataset, samples were from confirmed virus-positive volunteers during human infection challenge studies with RSV; the volunteers were 20–29 years old and mixture of female and male. The adult blood samples were taken at day 0 and day 7 of RSV challenge. Lastly, we collected blood from female BALB/c mice aged between 6 and 8 weeks on day 0 and day 7 of RSV infection. Characteristics and sample size for all datasets are in Table 1.

First, we examined the global transcriptomic response in whole blood from children, adults and mouse using principal component analysis (PCA). Across all three datasets, the PCA plots indicate consistent separation of infected from not infected; either cases from controls or earlier (pre-infection) from later (infected) time points. Of note, the timing of the blood sample collection relative to infection in children is different to the adults and the mice because the former samples are derived from natural infection studies meaning exact infection dates are unknown. Despite this, a clear separation between control and RSV hospitalised children was observed on PC1 (Fig. 1A). In children, genes that drove the separation of the two clusters mapped to GO pathways in DNA metabolic process (FDR = 1e−10), organelle organisation (FDR = 9e−16) and cell cycle (FDR = 4e−11). When the children with RSV were compared to controls (Fig. 1B), 3003 genes were differentially expressed (1339 genes over-expressed and 1664 genes under-expressed; FC > 0 and adjusted *P*-value < 0.1, Table 2). This constituted 40% of the total transcripts after filtering. In mice, samples from naïve and infected mice separated by PCA (Fig. 1C). 495 genes were significantly differentially expressed (338 genes over-expressed and 157 genes under-expressed; FC > 0 and adjusted *P*-value < 0.1, Fig. 1D). PCA separation was driven by neutrophil degranulation (FDR = 8.15 e-03), immune system (FDR = 1.13e−02) and antigen processing-cross presentation (FDR = 6.77e−04). Paired blood samples collected from adults comparing the day of challenge (day 0) and peak of symptoms (day 7) separated by PCA (Fig. 1E). Here, 12.4% of the total transcripts were differentially regulated, with 563 over-expressed and 798 under-expressed genes (Fig. 1F). PCA separation was driven by defence response (FDR = 6e−24), immune response (FDR = 2e−20) and response to external stimulus (FDR = 8e−19).

We then compared all genes across the three systems. Because not all genes map directly between human and mouse data, we used Gene Symbols and selected only genes that were present in both human and mouse and considered them “orthologs”. Whilst weak, the tightest correlation was observed between adult blood and children blood (R^2 = 0.101, $P = 2.1 \times 10^{-7}$) following RSV infection than that with children and mouse (R^2 = 0.074, $P = 1.7 \times 10^{-4}$) (Fig. 1G). The transcriptomic response in adult and mouse blood had the weakest correlation, sharing the fewest similarities. Gene function classification analysis was performed to study the over-expressed biological function of the blood DEGs shared across the aforementioned adult, child and mouse analyses (Fig. 1B, D and F), grouping them into GO terms (Fig. 1H). All three systems shared similarities with over-expressed pathways reflecting inflammation including the pathways: Response to Interferon Alpha, Response to Interferon Beta and Response to Cytokine all prominent. The most enriched GO pathway identified in adult blood was Interleukin-27-Mediated Signaling Pathway, in mice it was Response to Interferon Beta. Mouse and adults shared 80 genes which included over-expressed *OAS2, CD177 and IFGR2* (Fig. 1I). Children and mouse shared the fewest genes; the overlapped over-expressed genes including *CXCL10, VCAN, FN1, S100A8/S100A9* (Fig. 1J). In terms of individual genes, there were four common significantly over-expressed genes across all three datasets, these were *RTP4, BST1, STAT1* and *TMEM40*; all of which are associated with the immune response. Overall, we can see similarities between the transcriptomic response in blood in human challenge volunteers, mice and naturally infected children; with a marked upregulation of immune response related genes.

Nasal mucosal transcriptome shares patterns between systems

Curettage and transcriptional profiling of the nasal mucosa can provide valuable insights into host-pathogen interactions at the primary site of infection that may drive disease outcomes. Here, we compared datasets generated by bulk RNA-Seq of nasal tissue collected from children, adults, and mice. In children, transcriptomic data was generated from RNA extracted from nasal scrapes from 24 children at the time of hospitalisation following infection with RSV. They had a median age of 0.33 years, with 10 male and 14 females. This cohort was compared to age matched controls. In adults, material was collected at day 0 and 7 from nine confirmed RSV positive human infection challenge volunteers. In mice, nasal mucosa was collected from control mice and RSV infected mice at d7 of infection.

In the nasal samples from children, we did not observe separation in transcriptomic responses by PCA plot on PC1 (33.1%) but

Table 1
Characteristics of datasets.

Species	Age	Tissue	#Samples	Comments	Time points	Reference last author
Human	Adult	Blood	Day 0 N = 9 Day 7 N = 9	Microarray	Day 0, Day 7	GS Ginsburg[32]
		Nasal scrape	Day 0 N = 9 Day 7 N = 9	Bulk RNAseq	Day 0, Day 7	C Chiu[46] (Day 0, Day 7 unpublished)
		Lung biopsy	Day 0 N = 5 Day 7 N = 5	Microarray	Day 0, Day 7	C Chiu Unpublished
	Children	Blood	Control N = 45 RSV positive N = 42	Bulk RNAseq	Upon admission	M. Kaforou
		Nasal mucosa curettage	Control N = 22 RSV positive N = 24	Bulk RNAseq	Upon admission	B Coates[31]
Mouse	6-7 weeks	Blood	Control N = 5 RSV positive N = 5	Bulk RNAseq	Day 7	J.S. Tregoning[25]
		Nasal mucosa	Control N = 5 RSV positive N = 5	Bulk RNAseq	Day 7	Unpublished/ current study
		Lung	Control N = 5 RSV positive N = 5	Bulk RNAseq	Day 7	J.S. Tregoning[25]

rather PC2 (13.2%) (Fig. 2A). PC1 was marked by RNA associated responses such as RNA processing (FDR = 2e−109), translation (FDR = 1e−79) and mRNA metabolic process (FDR = 5e−76). In comparison, PC2 was predominately cell activation (FDR = 3e−92), regulation of immune process (FDR = 5e−89) and leucocyte activation (FDR = 3e−93). A distinct separation by PCA was observed for nasal RNA across PC1 for mice (Fig. 2B) and adult (Fig. 2C), this was driven by immune response (FDR = 2e−142) and detection of chemical stimulus (FDR = 2e−99). In the dataset from children, 5255 genes were identified as DEGs (39.4% over-expressed, 60.6% under-expressed; Fig. 2D), 1253 genes were differentially expressed in mice (67.1% over-expressed, 33.6% under-expressed; Fig. 2E) and 8088 DEGs were identified in adults (34.8% over-expressed, 65.2% under-expressed; Fig. 2F).

Given the broad similarities in the over-expressed gene pathways between datasets, we next explored correlations between them. As with the blood we only selected ortholog genes that were present in both human and mouse. Performing correlation analysis with the overlapping orthologs between the systems (Fig. 2G), the gene set from nasal mucosa collected from children was similar to both adults ($R^2 = 0.741$, $P = 5 \times 10^{-10}$) and mouse ($R^2 = 0.731$, $P = 1.2 \times 10^{-9}$). GO analysis was performed to assess the functions over-expressed in the nasal mucosa of each system (Fig. 2H). This indicated a different pattern to that seen in blood. The terms observed as differentially expressed in adult nasal mucosa were different to those in children and mice. Several pathways were strongly over-represented in RSV infected children and RSV infected mice, including Upregulation of Neutrophil Extracellular Trap Formation, B Cell Activation, T Cell Activation and IL-17 Signaling Pathway. 41 genes were concordant between adults and mouse, including *CCL5*, *IFIT1*, *GBP4* and *TNF* (Fig. 2I). 325 genes were shared between children and mouse; over-expressed genes in concordance included S100A8, *GZMB*, *CXCL9*, *CXCL10*, and *ACOD1* (Fig. 2J). 40 genes were commonly over-expressed in all three systems: children, adult and mouse.

The transcriptome of the lung is similar between adult humans and mice

We next compared the response in the lung tissue of the adults and mice following RSV infection. Due to size, practical and ethical restrictions, it was not possible to collect lung material from children. Endobrachial biopsies were collected from n = 5, RSV-positive volunteers on d0 and d7 of infection. Mouse lung samples were collected from control mice and infected mice on d7 of RSV infection.

The clear separation of mouse timepoint samples on PC1 (Fig. 3A) was driven by the following gene families: cytokine production (FDR = 1e−01), immune system process (FDR = 2e−01), and defence response (FDR = 2e−01). A clear separation was also observed between day 0 and day 7 of human RSV challenge in adults (Fig. 3B). It was driven mostly by PC1, consisting of genes in the axoneme assembly (FDR = 1e−18), cilium organisation (FDR = 1e−13) and cilium assembly (FDR = 2e−12) families. There were an overwhelming 20,000 mouse genes considered as DEGs (Fig. 3C), but only 740 DEG in the adult human lung RNA following infection (Fig. 3D).

Biological pathways over-expressed in adult lung data at day 7 of RSV infection were primarily innate response focused. As seen in blood, one of the major paths was the Interleukin-27 Related Signaling Pathway (Fig. 3E). There were also upregulations in Toll-like Receptor Signaling Pathways (for TLR2, 3 and 5). In contrast in mice, the GO terms Interleukin-6 Production and Cytokine Production were over-expressed. There were 30 overlapping over-expressed genes between the two systems (Fig. 3F) including those related to antiviral innate immunity (*ACE2, TLR1*), a Type I IFN receptor repressor (*USP18*), and a copper transporter *SLC31A1*.

Cross system and tissue comparison analysis identifies IL-17 as a pathway associated with disease

Having compared the different experimental models, we then compared responses between tissue types within the same models. In adults, the strongest correlation was observed between blood and lung ($R^2 = 0.672$, $P = 0.068$), followed by lung and nasal ($R^2 = 0.633$, $P = 0.093$) and blood and nasal mucosa ($R^2 = 0.368$, $P = 37$), however, these correlations were not statistically significant (Fig. 4A). This suggests that in an immunologically mature host immune responses to RSV are different between upper and lower respiratory tract. Only 3 differentially expressed genes overlapped between blood, nasal mucosa and lung in adults challenged with RSV at the peak of symptoms compared to the day of challenge: *USP18*, *IRF9* and *ISGF3* (Fig. 4B). More over-expressed genes were shared between blood and nasal mucosa, suggesting they share a more similar transcriptomic response. A network analysis was performed using InnateDB database to explore the genes associated with the three shared genes (Fig. 4C). Interestingly, *USP18* was associated with antiviral ISGs such as *IFIT1*, *IFIT3*, *MX1*, *MX2*, *IRF7* and *OASL*. And the *ISGF3* complex connected a large network of STAT proteins.

Likewise, the response to RSV in mouse blood was more like the nasal mucosa transcriptome ($R^2 = 0.455$, $P = 1.3 \times 10^{-5}$) than the lung ($R^2 = 0.123$, $P = 0.258$) (Fig. 4D). There was a significant correlation between mouse nasal mucosa and lung signatures ($R^2 = 0.345$, $P = 0.001$). There were 318 genes over-expressed in common between the two tissue types (Fig. 4E). 49 genes were considered as a core infection response shared between blood, nasal mucosa and lung. The key network from the core genes highlighted hub genes

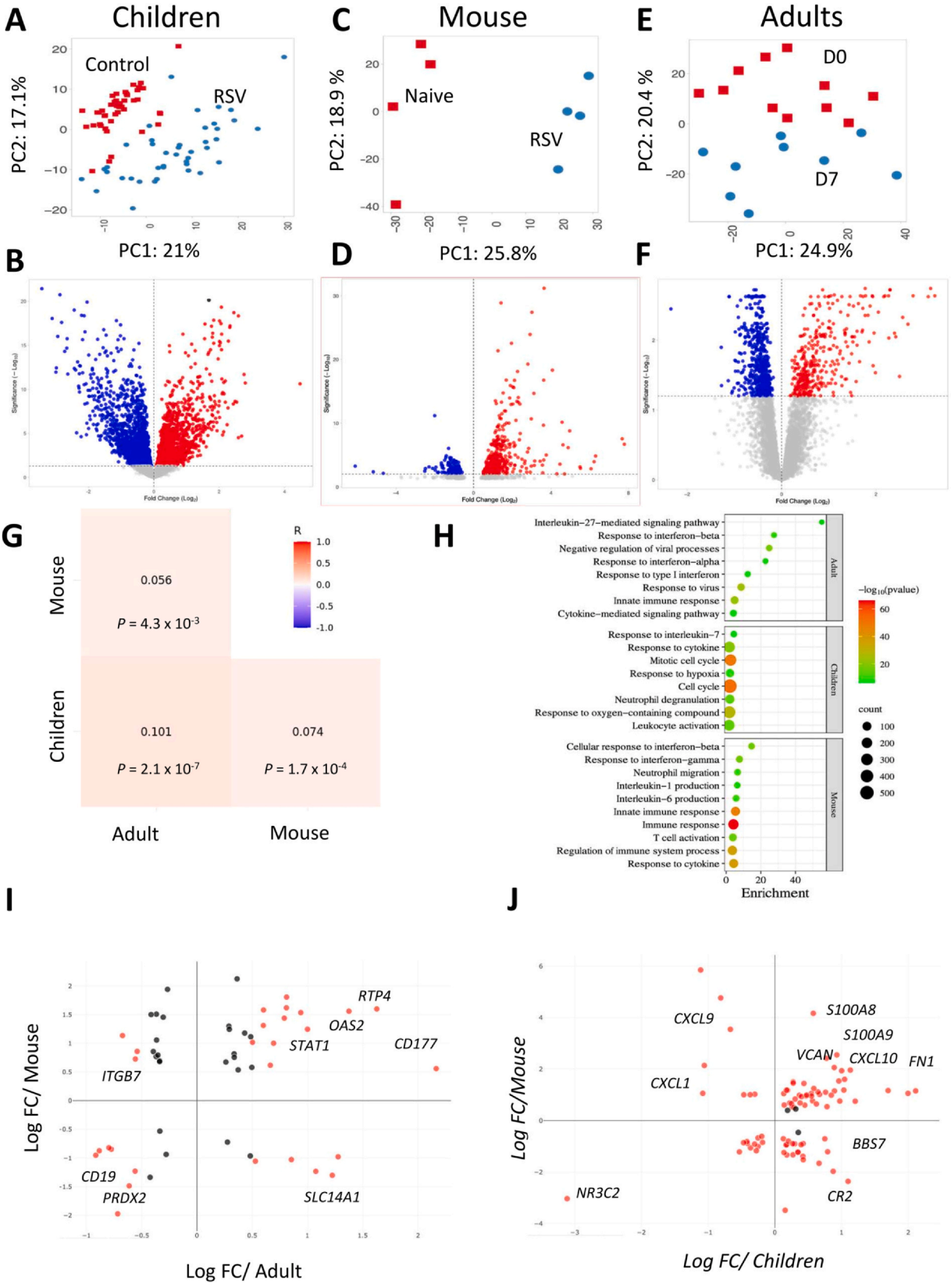


Fig. 1. Blood transcriptomes following RSV infection show limited similarities between systems. Principal component analysis (A, C, E) and volcano plots (B, D, F) showing differentially expressed genes (DEGs) were plotted for: (A, B) children (control (n = 45) and RSV (n = 42)), (C, D) mouse (naïve (n = 4) and RSV (n = 4)) and (E, F) adults (baseline (n = 11) and peak of symptoms (n = 9)). Red indicates over-expressed DEGs in response to RSV, blue indicates under-expressed DEGs. G) Correlogram was plotted for the entire dataset between children, mouse and adults. Number indicates the correlation coefficient (R). *P* value is indicated below. H) Over-expressed DEGs were taken for GO term analysis in biological processes. Enrichment score is shown along the X axis. Disco plots for each comparison: I) mouse and adult and J) mouse and children; Red dots satisfied all three criteria "$P < 0.05$, FDR < 0.1, $|FC| > 0$" in both datasets, Black dots satisfied all three criteria in one dataset (so either mouse or adult or children).

Table 2
Differentially expressed genes in respective datasets.

Species	Age	Tissue	Total transcripts after filtering	DEGs	Over-expressed	Under-expressed
Human	Adults	Blood	10,958	1361	563	798
		Nasal scrape	20,075	8088	2817	5271
		Lung biopsy	17,367	688	128	560
	Children	Blood	6424	3003	1339	1664
		Nasal mucosa curettage	14,330	5255	2070	3185
Mouse	6–7 weeks old	Blood	12,702	495	338	157
		Nasal mucosa	18,000	1253	841	412
		Lung	23,841	2,0718	5278	15,440

including *PTPN11, PTPN2, STAT3, JAK1, SOX9, IL21R, IL2RG* and *ITGB1BP1* (Fig. 4F). We next wanted to compare mouse to adult across blood, nasal mucosa and lung using over-expressed DEGs (Fig. S1).

Having explored adult and mouse models, we next explored the core response seen in child blood and nasal mucosa. There were 207 over-expressed genes (out of 746 ortholog genes) present in both tissue types. These genes included genes in both tissue types included *IFI44L, CXCL10, S100A8*, *S100A9*, *S100A12*, *SLC39A8* and *TNFAIP6* (Fig. 4G). When grouped by functional pathways, ZBP1 pathways were highly enriched, but so also was the Interluekin-17 Production pathway (Fig. 4H). We compared core overlapping responses to infection in blood and nasal between children, mouse and adults following RSV infection (Fig. 4I). All three systems shared increases in TLR signalling response and NF-KB signalling cascade. Notably, both children and mouse had significant increases in IL-17 pathways, suggesting they are involved in pathogenesis of severe disease to a primary RSV infection. DEGs associated with IL-17 production were screened in the blood of children and mouse, and many genes overlapped (Fig. 4J); *CEBPB*, *CXCL10*, *IL1B* were over-expressed in both systems and notably the genes *S100A8*/*A9* downstream of the IL-17A/F pathway were also highly expressed.

Blocking S100, the downstream effector of IL-17, reduces disease following RSV infection in mice

In the transcriptomics data, we observed an association between IL-17 production pathways and disease in both mouse and children. To confirm that this signalling pathway was playing a functional role during RSV infection, we used an *in vivo* mouse model. Mice were treated with neutralising antibodies targeting IL-17A, IL-17F, and as a cocktail IL-17A/F intraperitoneally on days −1, 2 and 5 after RSV infection at day 0. Control mice were injected at the same time with an IgG isotype control antibody. No weight loss was observed in the naïve group whilst RSV infected control mice had stable weight until day 4 and lost significant weight on days 5, 6 and 7 after infection compared to naïve (Fig. 5A). No difference was observed between RSV with αIL-17A treatment or RSV with αIL-17F treatment until day 6. On day 7, mice treated with αIL-17A mAb had started recovering weight compared to the RSV control group. αIL-17F alone had no significant impact on weight loss. However, when both IL-17A and IL-17F were neutralised together, mice lost more weight on day 3 compared to the control group but recovered faster on day 6 and 7. This weight change was reflected by reduced food consumption (Fig. 5B). The αIL-17A mAb treated mice also had significantly less viral RNA recovered from the lungs on day 7 after infection (Fig. 5C). RSV infected mice had more $CD4^+$ T cells recruited to the lungs on day 7 after infection than naïve mice, there was no difference following antibody treatment (Fig. 5D). However, there was a significant reduction in the number of RSV^+CD8^+ cells in the lung in the αIL-17A mAb treated mice (Fig. 5E). Comparing cytokine responses by intracellular staining, there was no difference in the amount of $CD4^+$ T cells producing IL-17A across all infected groups (Fig. 5F), but there were slightly more $CD8^+$ T cells producing IL-17 after infection compared to naïve groups (Fig. 5G). Levels of IgG were also lower in α-IL-17A/F treated groups compared to the control (Fig. 5H).

Our studies neutralising IL-17 validate a role for this pathway in primary RSV disease and open up opportunities for novel interventions. Two genes in the IL-17 pathway over-expressed after RSV infection in mice and children were *S100A8* and *S100A9* (Fig. 4J). The drug paquinimod was developed to block the action of S100A9 in SLE; it has been tested during murine infection with SARS-CoV-2[11] but not RSV. 12.5 μg Paquinimod was given intranasally at day −1, 1, 2, 3 and 5 following RSV infection at day 0; the control group received PBS. Mice receiving Paquinimod recovered faster after RSV infection than control mice (Fig. 5I), but there was no difference in food consumption (Fig. 5J). Interestingly the treated mice had significantly lower viral load (Fig. 5K), but no difference in antibody responses (Fig. 5L). This shows that the comparative transcriptomic approach can be used to identify novel targets and therapies for RSV disease.

Discussion

Here we set out to triangulate systems comparing different RSV transcriptomic datasets to identify novel pathways in RSV disease pathogenesis. The data was collected from three tissue types, lung, nasal mucosa and blood from natural RSV infection of children, adult human challenge and BALB/c mouse *in vivo*. In the blood transcriptome, there were concordant gene expression patterns between adults and children in pathways associated with inflammation. When we compared primary infection (children and mice), we observed increased expression in the IL-17 pathway. Drilling down into this pathway, we observed upregulation of the genes *S100A8* and *S100A9*, which when blocked with the anti-inflammatory drug Paquinimod reduced disease. Therefore, this cross system 'omics approach identifies novel approaches to reduce disease following RSV infection.

There are some limitations that need to be considered. Studies of adults included both male and females due to limited participant numbers, likewise the nasal transcriptome in children was also a mixture of male and female participants; whereas the child blood dataset and mice were only female. This confounding factor should be taken into account as sex is an important biological variable that affects the functions of the immune system.[12] There was a wide age range in the children included, which could explain some of the variation observed. Although participants in all studies were confirmed to be RSV positive by PCR and negative for common respiratory viruses such as flu and rhinoviruses, there was no screening for bacterial infections in the clinical studies. The samples for different tissues were not collected from the same individuals; and because it was destructive sampling, mouse samples were compared to uninfected controls. Lastly, differences in the blood counts in the children, adult and mice models were not normalised to the lymphocyte counts. We chose not to carry out this step as it was necessary to maintain the true differences that naturally existed

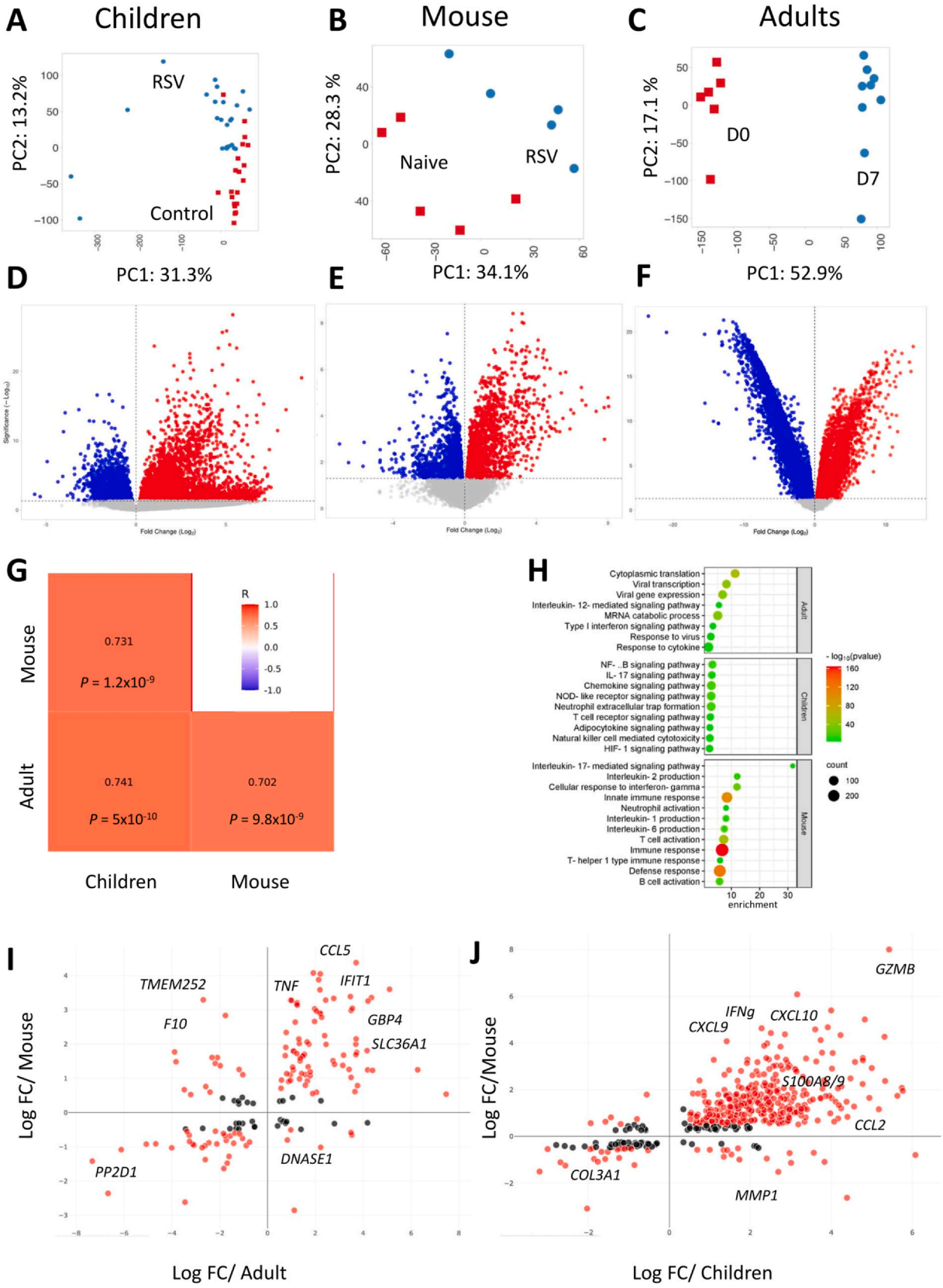


Fig. 2. Nasal transcriptome shares patterns between systems. Principal component analysis (A, B, C) and volcano plots (D, E, F) showing differentially expressed genes (DEGs) were plotted for: (A, D) children (control (n = 20) and RSV (n = 24)), (B, E) mouse (naïve (n = 5) and RSV (n = 5)) and (C, F) adults (baseline (n = 6) and peak of symptoms (n = 9)). Red indicates over-expressed DEGs in response to RSV, blue indicates under-expressed DEGs. G) Correlogram of overlapped ortholog genes, between children, mouse and adults. Number indicates the correlation coefficient (R), *P* value was indicated below. H) Over-expressed DEGs were taken for GO term analysis in biological processes. Enrichment score is shown along the X axis. Disco plots for each comparison: I) mouse and adult and J) mouse and children; Red dots satisfied all three criteria "P < 0.05, FDR < 0.1, |FC| > 0" in both datasets, Black dots satisfied all three criteria in one dataset (so either mouse or adult or children).

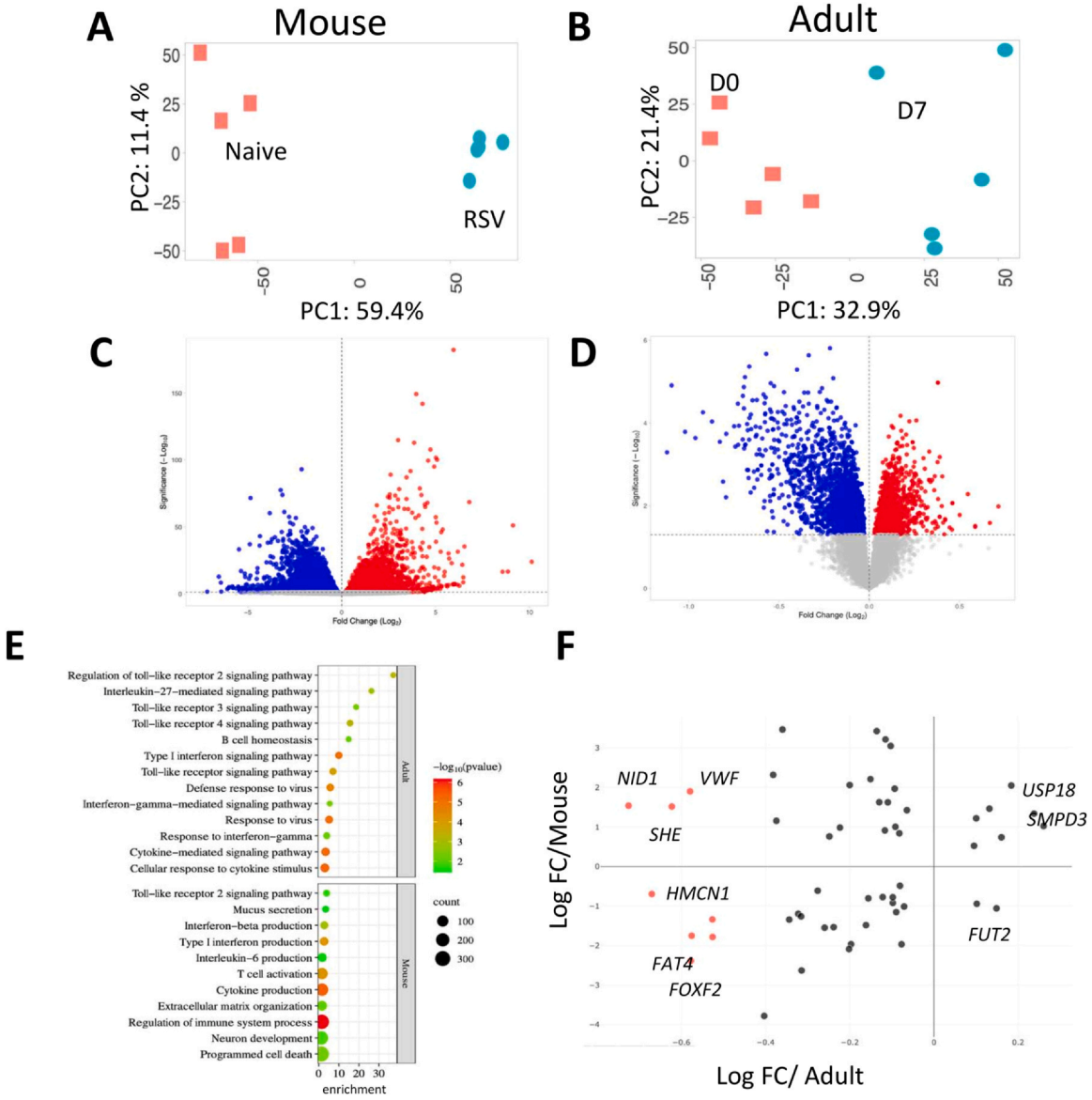


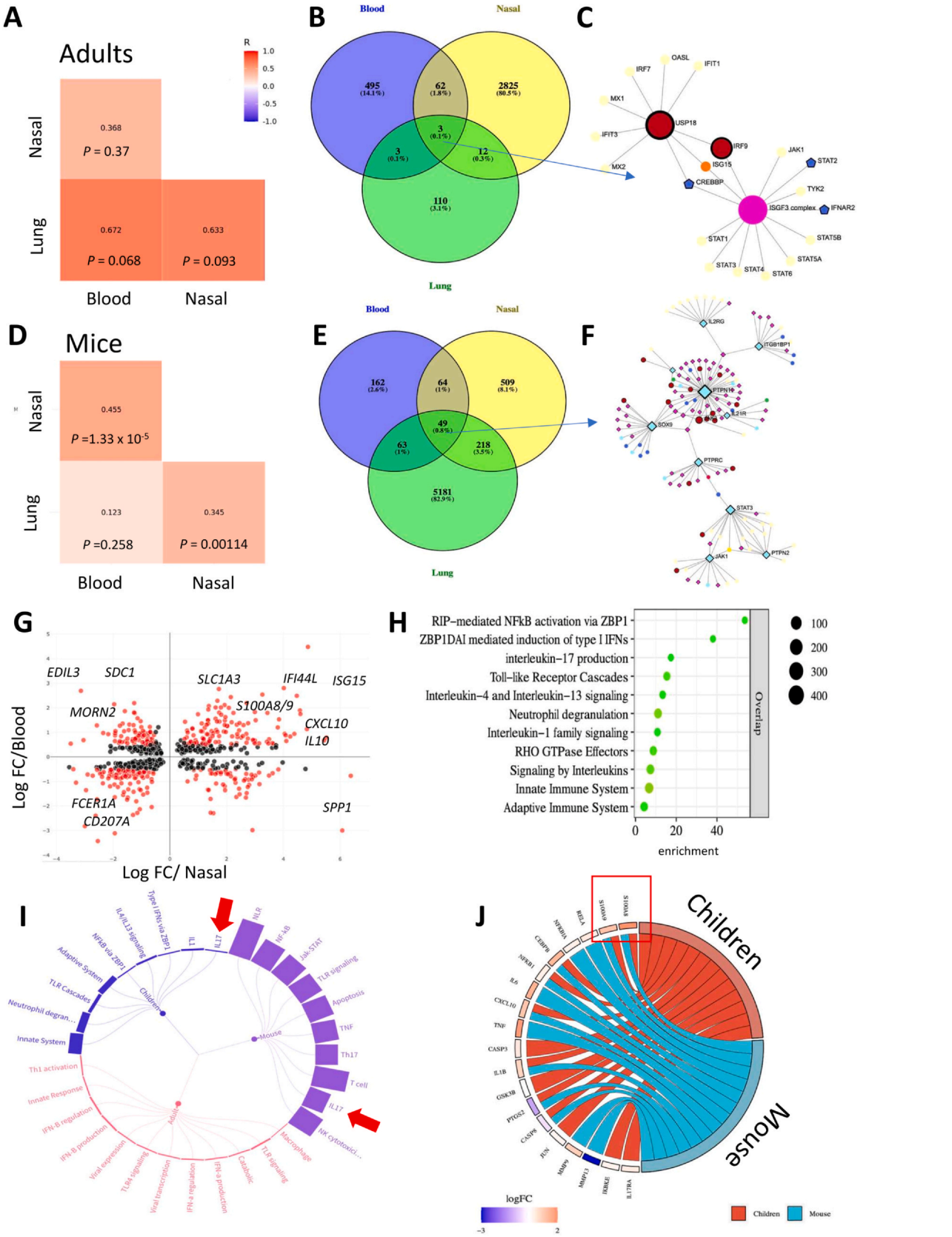
Fig. 3. The transcriptome of the lung is similar between adult humans and mice. Principal component analysis (A, B) and volcano plots (C, D) showing differentially expressed genes (DEGs) were plotted for (A, C) mouse (naïve (n = 5) and RSV (n = 4)) and (B, D) adults (baseline (n = 5) and peak of symptoms (n = 5)). Red indicates over-expressed DEGs in response to RSV, blue indicates under-expressed DEGs. E) Over-expressed DEGs were taken for GO term analysis in biological processes. Enrichment score is shown along the X axis. F) Disco plot was used to compare genes differentially regulated in the same direction in mouse and adults; Red dots satisfied all three criteria "$P < 0.05$, FDR < 0.1, $|FC| > 0$" in both datasets, Black dots satisfied all three criteria in one dataset (so either mouse or adult or children).

in each system. In spite of the heterogenous datasets, it is notable that we observed considerable overlaps in the response to infection, indicating the value of the approach.

Looking at the models separately we observed that in children with RSV, neutrophils and hypoxia were core pathways in the blood and nasal transcriptomes. Response to hypoxia has been recently reported to contribute to clinical disease and the control of viral replication during RSV infection.[13] Consistent with previously published work, neutrophils are a hallmark of severe disease in infants with RSV. This was also detected in the mouse datasets. However, the depletion of neutrophils did not impact viral load or the peak of disease in mouse models during infection.[14] This could be explained by our data where mouse responses to RSV were dominated by other arms of the immune response such as T cell activation. Further similarities between children and mouse exist when cytokine responses were compared. *IL-6, IL-18R1, CXCR6* and *IL-1* were significantly over-expressed in both blood and nasal transcriptomes.

Network analysis provided further insights, particularly concerning unique processes in adults that were absent in children and mouse. A systemic upregulation of the IL-27 related pathway was observed in the lung and blood of adult challenged with RSV on day 7. IL-27 is a heterodimeric cytokine known for its effects on T-cell function and differentiation. IL-27 signals through the IL-27 receptor (IL-27R) which activates STAT1 signalling, induces the expression of the type 1 helper T cell (Th1) cytokine, and suppresses the differentiation of Th2 and Th17 cells. IL-27 has been shown as a major regulatory mediator produced by lung resident immune cells, which in turn drives suppression of otherwise damaging inflammation.[15] Previous studies have observed an interplay between IL-27 and IL-17[16]; disease exacerbation marked by increased mucus secretion was observed in the lungs from RSV-infected IL-27rKO mice compared to wild type.

When we compared systems, we observed a significant upregulation of the IL-17 signalling pathway in children and mouse, which



(caption on next page)

Fig. 4. Cross system and tissue comparison analysis identifies IL-17 as a pathway associated with disease. A) Correlogram was plotted for overlapped genes present between lung, nasal and blood in the adults. Number in the box indicated the correlation coefficient (R), with Pearson's *P* values indicated below. Over-expressed genes overlapping in each tissue type were shown in the Venn diagram (B) and the three genes presented in all three types were used in the network analysis (C). D) Correlogram was plotted for overlapped genes present between lung, nasal and blood in the Mouse. Number in the box indicated R, with Pearson's *P* values indicated below. Over-expressed genes overlapping in each tissue type were shown in the Venn diagram (E) and the three genes presented in all three types were used in the network analysis (F). G) Disco plot to compare children blood and children nasal mucosa; Red dots satisfied all three criteria "$P < 0.05$, FDR < 0.1, $|FC| > 0$" in both datasets, Black dots satisfied all three criteria in one dataset (so either mouse or adult or children). H) GO term analysis of over-expressed genes in blood, nasal and overlapped genes. I) Chord diagram of core pathways identified in children, mouse and adults were selected here to identify common pathways across species. J) Gene differentially expressed in the IL-17 pathway in children was selected identify common counterparts with mouse.

was absent in adults. Nasal concentrations of proinflammatory IL-17A are higher in infants requiring ventilation[17] and elevated IL-17 is a marker of more severe bronchiolitis.[18] Linking with the observation that neutrophils are associated with RSV disease, tracheal IL-17A concentrations positively correlate with neutrophil counts.[19] Neutralising IL-17 with monoclonal antibodies reduced weight loss, indicating improved disease outcomes. Our findings confirm previous studies that have identified a role for IL-17A in RSV disease.[20–22] Interestingly we observed a difference between IL-17A and IL-17F blockade; neutralising IL-17A significantly reduced RSV viral load in the lung but blocking IL-17F did not. The functional differences between IL-17A and IL-17F might be because IL-17A binds to IL-17 receptor A (IL17RA) and IL-17RC, but IL-17F binds to IL-17RA and IL-17RF.[23] Potentially IL-17A is also altering behaviour by binding receptors in the brain[24]; we have seen a similar effect for IL-1α altering appetite.[25]

IL-17 induces a signalling cascade, and recruitment and activation of other cells particularly neutrophils, we therefore explored whether within the IL-17 pathway, there were possible targets to reduce disease. Amongst the over-expressed genes in both children and mice were MMP-13, activated by neutrophils[26] and MMP-9, secreted by neutrophils.[27] MMP-9 during RSV infection has been targeted with Azithromycin in a previous clinical trial, but no effect was seen on long term outcomes.[28] Two other genes from the IL-17 pathway associated with neutrophils are *S100A8*/*A9*, members of the S100 group of proteins. The major functions of S100A8/A9 reported so far include the regulation of leucocyte migration and trafficking, the remodelling of cytoskeleton and amplification of inflammation,

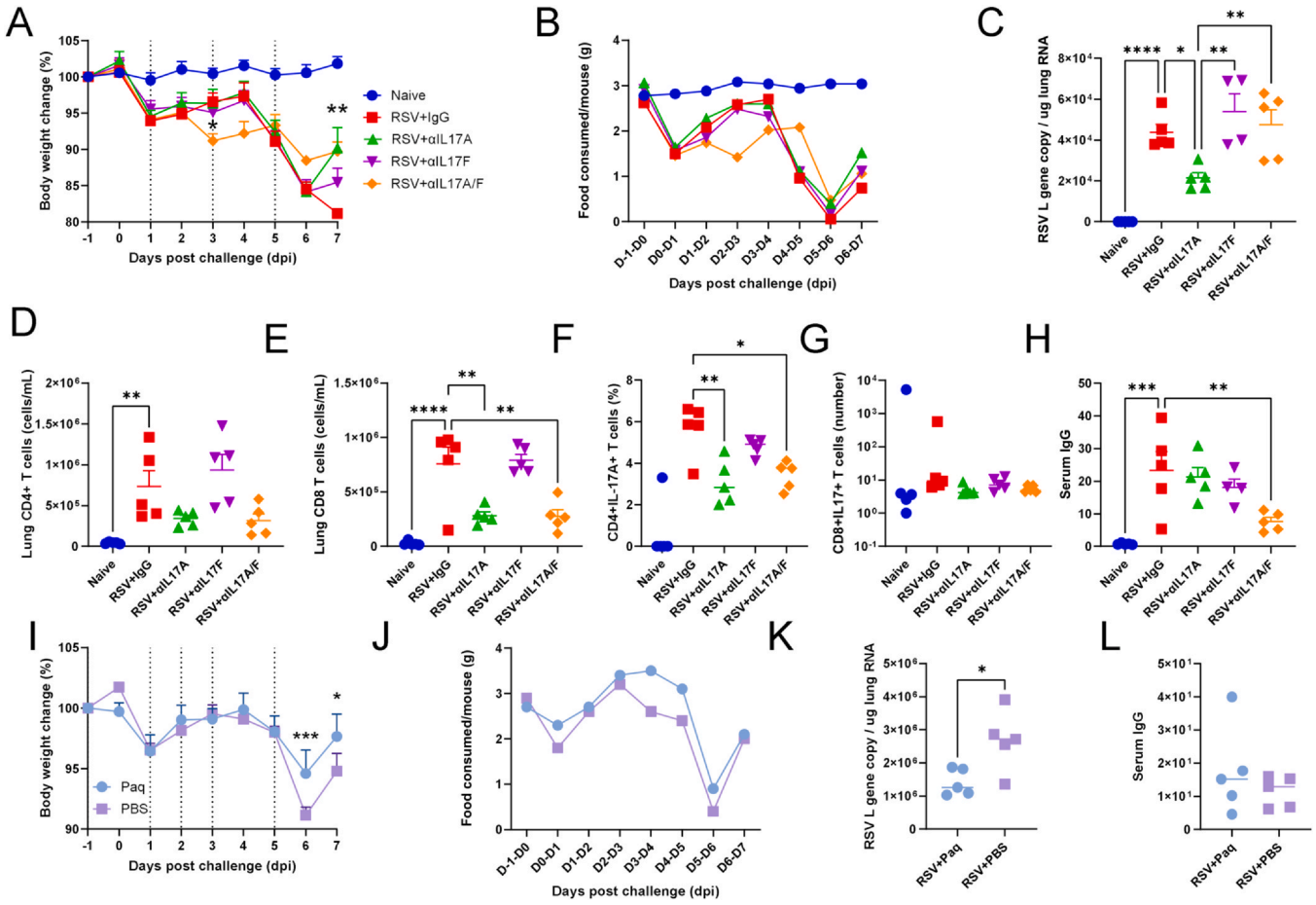


Fig. 5. IL-17 and the downstream effector S100 contribute to disease following RSV infection in mice. 6–7 weeks old female BALB/c were intranasally infected with 7.7×10^6 RSV subtype A on day 0 and intraperitoneally injected with 500 μg of monoclonal antibody targeting IL-17A, IL-17F, IL-17A/F or IgG on day −1, 1, 3 and 5 post RSV infection. Naïve group received no treatment. A) Body weight and B) food consumed were monitored daily. C) Viral load was performed using qPCR to measure RSV L gene. Flow cytometry was carried out to identify total cell count: D) $CD4^+$, E) $CD8^+$. Intracellular staining was carried out to stain for IL-17A in F) $CD4^+$ and G) $CD8^+$ T cells. H) Serum IgG was measured using ELISA. 6–7 weeks old female BALB/c was intranasally infected with $7.7. \times 10^6$ RSV subtype A on day 0 and intranasally administered with Paquinimod S100A8/S100A9 on day −1, 1, 3 and 5 post RSV infection. I) Body weight and J) food consumed were monitored daily. K) Viral load was measured using qPCR to quantify RSV L gene. L) Serum anti-RSV IgG level was measured using ELISA. N = 5, each dot represents an individual mouse (C–H, K–L); or mean +/-SEM (A, B, I, J). Significance calculated by ordinary one-way ANOVA and post-test. $^*P \leq 0.05$, $^{**}P \leq 0.01$, $^{***}P \leq 0.001$. ICS staining analysed using FLOWJO.

and exertion of anti-microbial activity.[11] In a study of *Mycoplasma pneumoniae*-induced pneumonia, IL-17 was shown to stimulate neutrophils to release S100A8/A9 to promote lung epithelial cell apoptosis.[29] Paquinimod (a Laquinimod derivative) is an orphan immunomodulatory drug that was developed to treat systemic lupus erythematosus.[30] It has been observed to reduce disease following SARS-CoV-2 infection.[11] We therefore explored whether it could also reduce RSV disease; mice receiving Paquinimod recovered faster, validating our approach for the identification of new drug targets. This comprehensive comparative study provides insights into common and species-specific processes underlying RSV infection. The identification of key pathogenesis processes and the discovery of host factors facilitate the development of therapeutic interventions against RSV.

Materials and methods

Datasets

Characteristics of datasets described in Table 1.

Child transcriptomics

Blood transcriptomic data from children were derived from the Diagnosis and Management of Febrile Illness using RNA Personalised Molecular Signature Diagnosis (DIAMONDS consortia). Venous blood was collected from patients at the time of hospitalisation and stored in PAXgene Blood RNA. RNA-Seq was carried out at The Wellcome Centre for Human Genetics in Oxford, United Kingdom, using a Novaseq600 platform at 150 bp paired-end configuration, generating a raw read count of 30 million reads per sample. The normalised dataset is available in ArrayExpress (E-MTAB-12793). 45 controls and 42 RSV positive samples were included.

In a separate study,[31] nasal mucosa curettage was performed and obtained from 22 healthy children (less than 18 years of age) and 24 children (median age 0.33 years old, 10 male, 14 females) infected with RSV at Ann and Robert H. Lurie Children's hospital of Chicago. RSV infection was confirmed by a PCR test and children were admitted to the paediatric intensive care unit with symptoms of pulmonary parenchymal disease. RNA sequencing was performed on a NextSeq 500 instrument (Illumina), 75 cycles, single-end, to an average sequencing depth of 5.88 M reads.

Adult human challenge transcriptomic data

Adult human samples came from controlled human infection challenge studies.

For blood samples, previously published data was used[32]; microarray data was derived from 9 symptomatic volunteers infected with 10^4 $TCID_{50}$ RSV.

For nasal scrape and endobronchial biopsy, healthy, non-smoking adults aged 20–29 years old both female and male were included. Inclusion/exclusion criteria are the same as previous studies[33]; participants were enroled without preselection by anti-RSV antibody concentrations. Participants were inoculated with 10^4 plaque-forming units (PFU) of RSV A Memphis-37 (M37) by intranasal drops and quarantined for 10 days post inoculation. Nasal washes and bronchoscopy samples were collected at d0 and d7 of infection. Participants were selected from larger studies based on positive infection with RSV (defined by PCR positivity); nasal scrapes were collected from 9 donors, lung biopsies from 5 donors. Nasal scrape data were processed by RNASeq, bronchoscopy by microarray.

Animal studies

6–8-week-old female BALB/c specific-pathogen-free (SPF) mice were purchased from Charles River Laboratories (Helston, U.K.) and maintained according to institutional and United Kingdom Home Office guidelines. All experiments were performed in the SPF room in the animal facility on a 12-h light/dark cycle at 20–24 °C with 55% ± 10% humidity. All work was approved by the Animal Welfare and Ethical Review board at Imperial College London, and studies were in accordance with the Animal Research: Reporting of *In vivo* Experiments (ARRIVE) guidelines.

Mice were housed in groups of five animals per cage. For all infection studies, mice were anaesthetised using 2.5% of isoflurane and intranasally (i.n.) infected with 7.7×10^6 PFU RSV subgroup A2 in 100 µL. Animal weight was measured daily after infection, as well as weight of food in hopper.[34] For IL-17 blockade, 500 µg of αIL-17A (BioXCell: BE0173), αIL-17F (BioXCell: BE0303), or αIL-17A/F monoclonal antibody cocktail was intraperitoneally injected on days −1, 2 and 5 after RSV infection at day 0. For S100 blockade, 12.5 mg Paquinimod (TargetMOI: T7310) was given intranasally at day −1, 1, 2, 3 and 5 following RSV infection at day 0.

Mouse tissue collection and RNA extraction

Blood was collected by cardiac puncture and mixed with PAXgene solution. RNA extracted using the PAXgene blood RNA kit according to the manufacturer's instructions (Qiagen).

Lungs were removed after dissection and the left lobe snap frozen for future RNA extraction. RNA was extracted from the lung lobe by first homogenising the tissue in 2 mL tubes containing ball bearings and 350 µL TRIzol reagent using a TissueLyzer at 50 oscillations for 4 min.

For nasal tissues, isolated mice heads were immediately dissected to extract nasal mucosal membrane from the nasal cavity as previously described[35] and extraction was carried out in the TissueLyzer at 50 oscillations for 8 min.

Mouse flow cytometry

The right mouse lobe was processed for flow cytometry as previously described.[36] After manual dissociation, cells were stained with Live/Dead dye, prior to resuspension in Fc Block in PBS-1% BSA. Cells were then stained with surface antibodies, prior to intracellular staining and fixing in 0.5% PFA. Each sample was filtered through the FAC tubes before running on an LSR Fortessa Flow cytometer (BD). Fluorescent minus one (FMO) controls were used for surface stains. Analysis was performed using FlowJo (Sample plot Fig. S2).

Mouse qPCR for RSV load

Lung RNA concentrations were determined using a Nanodrop before converting into cDNA using GoScript reverse transcription system using 2 µg for all samples. qPCR for the RSV L gene was performed on a Stratagene Mx 3005p (Agilent Technologies, Santa Clara, CA, USA) using the primers 5′-GAACTCAGTGTAGGTAGAATGT TTGCA-3′ and 5′-TTCAGCTATCATTTTCTCTGCCAA-3′ and probe 5′-6-carboxyfluorescein (FAM)-TTTGAACCTGTCTGAACAT-6-carboxytetramethylrhodamine (TAMRA)-3′.[37] RNA copy number per mg of lung RNA was determined using an RSV L gene plasmid standard (10^1–10^8 copies).

Pre-processing of sequencing data

Quality of Raw RNAseq reads generated was assessed using FastQC (v0.11.9) to ensure good quality scores, GC content and no adaptor reads, then appropriate adjustments were made using the

programme Trimmomatic (v1.0.40).[38] This included the following operations: Illumina universal adaptors were removed with ILLUMINACLIP, reads with an average quality score of less than 20 across a window of 4 bases were trimmed using sliding window, reads less than 20 bases in length were removed. FastQC was performed again on trimmed reads. Raw reads were then mapped to Mouse Reference Genome (Gmc38) using RNA STAR (Spliced Transcripts Alignment to a Reference, v6.2.0) and count data for each gene performed using featureCounts[39] (v1.2.0). For human RNAseq and microarray files, reads were aligned to the human reference genome GRCH39. Reads were filtered prior to expression analysis to remove any genes with a total read count of less than 5 across all samples. Principal component analysis (PCA) and heatmap visualisation on normalised data was analysed by the variance stabilising transformation method. R function prcomp() was used for PCA in the package Devtools(v2.4.2).

For pathway analysis from PCA plots, the PAGE algorithm performed one-sample *t*-test on each gene set in the biological processes branch of Gene Ontology (GO). The adjusted P-values were used to rank the pathways for each of the first two principal components. The duplicated pathways were skipped.

Heatmap visualisation was performed the heatmap.2 function in ggplot package (v3.1.1).[40]

Differential expression analysis

Limma package[41] was selected. DEGs were included if *P* values were less than 0.05 (FDR < 0.1) and fold change greater than 0 indicated overexpression; fold change less than 0 indicated under expression. No cut-off was selected to ensure genes with smaller fold changes which were biologically significant at large sample size, were included.

Gene ontology and KEGG network analysis

ClusterProfiler[42] was used to assess the enrichment of GO pathways in each gene list comparing the significantly expressed genes against background genes. Network analysis of the GO terms was analysed using the emapplot function in the clusterProfiler package. KEGG pathway was analysed using the gseKEGG function. Gene lists analysed include genes that were identified as significantly differentially variable and genes that were in a specific GO term. Gene set enrichment analysis (GSEA) was performed where enrichment score was calculated as the −log10 (*P*-value).[43] The network analysis of KEGG pathways (network visualisation and clustering) was performed with NetworkAnalyst.[44] R code is available upon request.

Concordant plots

Significantly differentially expressed genes present in both dataset were used in the concordant/discordant plot.[45] Discrete colours were played as −log10(Pvalue(X)), sizes were defined as −log10(Pvalue(Y))*(multiplier+2). Terms with NA in either dimension were excluded. Overlapping gene sets were compared on Venny2.0.

Statistics

All statistical analyses were performed in Graph Pad Prism V9 (GraphPad Software, San Diego, CA), R version 3.5.0. A statistically significant difference was defined as a *P*-value < 0.05 by one-way analysis of variance (ANOVA). Mouse data has been archived at ArrayExpress (RNASeq), human data available upon request.

CRediT authorship contribution statement

ZW: Data curation, Formal analysis, Visualisation, Investigation, Writing – original draft. CD: Data curation, Formal analysis, Investigation. PD: Data curation, Formal analysis, Investigation. SI: Investigation. MK: Conceptualisation, Supervision, Writing – editing. CC: Supervision, Writing – editing. JST: Conceptualization, Funding acquisition, Writing – review & editing.

Resource availability

Most of the RNA datasets discussed have been deposited in NCBI's Gene Expression Omnibus (GEO) and are accessible through the following GEO series accession number:

Adult blood GSE17156.

Adult Nasal GSE155237 (Day 0).

Adult Lung (TBC).

Children Blood (TBC).

Raw data for Children nasal was deposited to dbGap, under the accession number phs003053.v1.p1.

Mouse blood and lung can be found on Array Express, 38382577.

Funding

This work was funded in part by Department of Infectious Disease, Imperial College London as part of the Molecular and Cellular Basis of Infection program, in part by Wellcome Trust studentship and by an NIHR BRC award to Imperial supported JT and CC.

Declaration of Competing Interest

The authors declare the following financial interests/personal relationships which may be considered as potential competing interests: Ziyin Wang reports financial support was provided by Wellcome Trust. John Tregoning reports financial support was provided by NIHR BRC. If there are other authors, they declare that they have no known competing financial interests or personal relationships that could have appeared to influence the work reported in this paper.

Acknowledgements

The authors thank Kasia S for assistance in the *in vivo* studies, Lesley Rawlinson for lab management, Bria Coates for access to the child nasal dataset and Dr Stephanie Ascough for support on challenge studies.

For the purpose of open access, the author has applied a Creative Commons Attribution (CC BY) license to any Author Accepted Manuscript version arising.

Appendix A. Supporting information

Supplementary data associated with this article can be found in the online version at doi:10.1016/j.jinf.2026.106696.

References

1. Dapat C, Kumaki S, Sakurai H, Nishimura H, Labayo HKM, Okamoto M, et al. *Gene signature of children with severe respiratory syncytial virus infection. Pediatr Res* 2021;**89**:1664–72. https://doi.org/10.1038/s41390-020-01347-9
2. Agac A, Kolbe SM, Ludlow M, Osterhaus A, Meineke R, Rimmelzwaan GF. *Host responses to respiratory syncytial virus infection. Viruses* 2023;**15**:1999. https://doi.org/10.3390/v15101999
3. Davis MM, Tato CM, Furman D. *Systems immunology: just getting started. Nat Immunol* 2017;**18**:725–32. https://doi.org/10.1038/ni.3768
4. Box GEP. *Science and statistics. J Am Stat Assoc* 1976;**71**:791–9. https://doi.org/10.1080/01621459.1976.10480949
5. Habibi MS, Chiu C. *Controlled human infection with RSV: The opportunities of experimental challenge. Vaccine* 2017;**35**:489–95. https://doi.org/10.1016/j.vaccine.2016.08.086
6. Geerdink RJ, Pillay J, Meyaard L, Bont L. *Neutrophils in respiratory syncytial virus infection: a target for asthma prevention. J Allergy Clin Immunol* 2015;**136**:838–47. https://doi.org/10.1016/j.jaci.2015.06.034

7. Drysdale SB, Thwaites RS, Price J, Thakur D, McGinley J, McPherson C, et al. *What have we learned from animal studies of immune responses to respiratory syncytial virus infection? J Clin Virol* 2024;**175**:105731. https://doi.org/10.1016/j.jcv.2024.105731
8. Openshaw PJ, Tregoning JS. *Immune responses and disease enhancement during respiratory syncytial virus infection. Clin Microbiol Rev* 2005;**18**:541–55. https://doi.org/10.1128/CMR.18.3.541-555.2005
9. Writing Committee for the REMAP-CAP Investigators. *Long-term (180-day) outcomes in critically ill patients with COVID-19 in the REMAP-CAP randomized clinical trial. JAMA J Am Med Assoc* 2023;**329**:39–51. https://doi.org/10.1001/jama.2022.23257
10. Houben ML, Rovers MM, Wilbrink B, Belderbos ME, Bloemen-Carlier EM, Visser GH, et al. *High concentrations of amniotic fluid proinflammatory cytokines in healthy neonates are associated with low risk of respiratory syncytial virus bronchiolitis. Pediatr Infect Dis J* 2012;**31**:931–4. https://doi.org/10.1097/INF.0b013e31826366e3
11. Guo Q, Zhao Y, Li J, Liu J, Yang X, Guo X, et al. *Induction of alarmin S100A8/A9 mediates activation of aberrant neutrophils in the pathogenesis of COVID-19. Cell Host Microbe* 2021;**29**:222–35. https://doi.org/10.1016/j.chom.2020.12.016. .e224.
12. Klein SL, Flanagan KL. *Sex differences in immune responses. Nat Rev Immunol* 2016;**16**:626–38. https://doi.org/10.1038/nri.2016.90
13. Morris DR, Qu Y, de Mello AH, Jones-Hall YL, Liu T, Weglarz M, et al. *Hypoxia-inducible-factors differentially contribute to clinical disease and viral replication during RSV infection. bioRxiv* 2024. https://doi.org/10.1101/2023.08.15.553422
14. Kirsebom F, Michalaki C, Agueda-Oyarzabal M, Johansson C. *Neutrophils do not impact viral load or the peak of disease severity during RSV infection. Sci Rep* 2020;**10**:1110. https://doi.org/10.1038/s41598-020-57969-w
15. Pyle CJ, Uwadiae FI, Swieboda DP, Harker JA. *Early IL-6 signalling promotes IL-27 dependent maturation of regulatory T cells in the lungs and resolution of viral immunopathology. PLoS Pathog* 2017;**13**:e1006640. https://doi.org/10.1371/journal.ppat.1006640
16. de Almeida Nagata DE, Demoor T, Ptaschinski C, Ting HA, Jang S, Reed M, et al. *IL-27R-mediated regulation of IL-17 controls the development of respiratory syncytial virus-associated pathogenesis. Am J Pathol* 2014;**184**:1807–18. https://doi.org/10.1016/j.ajpath.2014.02.004
17. Faber TE, Groen H, Welfing M, Jansen KJ, Bont LJ. *Specific increase in local IL-17 production during recovery from primary RSV bronchiolitis. J Med Virol* 2012;**84**:1084–8. https://doi.org/10.1002/jmv.23291
18. Thwaites RS, Coates M, Ito K, Ghazaly M, Feather C, Abdulla F, et al. *Reduced nasal viral load and IFN responses in infants with respiratory syncytial virus bronchiolitis and respiratory failure. Am J Respir Crit Care Med* 2018;**198**:1074–84. https://doi.org/10.1164/rccm.201712-2567OC
19. Stoppelenburg AJ, von Hegedus JH, Huis in't Veld R, Bont L, Boes M. *Defective control of vitamin D receptor-mediated epithelial STAT1 signalling predisposes to severe respiratory syncytial virus bronchiolitis. J Pathol* 2014;**232**:57–64. https://doi.org/10.1002/path.4267
20. Stoppelenburg AJ, Salimi V, Hennus M, Plantinga M, Huis in 't Veld R, Walk J, et al. *Local IL-17A potentiates early neutrophil recruitment to the respiratory tract during severe RSV infection. PLoS One* 2013;**8**:e78461. https://doi.org/10.1371/journal.pone.0078461
21. Long X, Xie J, Ren L, Yu G, Liu E, Deng Y, et al. *IL-17A plays a critical role in RSV infection in children and mice. Virol J* 2023;**20**:30. https://doi.org/10.1186/s12985-023-01990-8
22. Liu X, Nguyen TH, Sokulsky L, Li X, Garcia Netto K, Hsu AC, et al. *IL-17A is a common and critical driver of impaired lung function and immunopathology induced by influenza virus, rhinovirus and respiratory syncytial virus. Respirology* 2021;**26**:1049–59. https://doi.org/10.1111/resp.14141
23. Mazur NI, Terstappen J, Baral R, Bardají A, Beutels P, Buchholz UJ, et al. *Respiratory syncytial virus prevention within reach: the vaccine and monoclonal antibody landscape. Lancet Infect Dis* 2023;**23**:e2–21. https://doi.org/10.1016/s1473-3099(22)00291-2
24. Lee B, Kwon JT, Jeong Y, Caris H, Oh D, Feng M, et al. *Inflammatory and anti-inflammatory cytokines bidirectionally modulate amygdala circuits regulating anxiety. Cell* 2025;**188**:2190–202. https://doi.org/10.1016/j.cell.2025.03.005. .e2115.
25. Wang Z, Cuthbertson LF, Thomas C, Sallah HJ, Mosscrop LG, Li H, et al. *IL-1α is required for T cell-driven weight loss after respiratory viral infection. Mucosal Immunol* 2024;**17**:272–87. https://doi.org/10.1016/j.mucimm.2024.02.005
26. Wilkinson DJ, Falconer AMD, Wright HL, Lin H, Yamamoto K, Cheung K, et al. *Matrix metalloproteinase-13 is fully activated by neutrophil elastase and inactivates its serpin inhibitor, alpha-1 antitrypsin: implications for osteoarthritis. FEBS J* 2022;**289**:121–39. https://doi.org/10.1111/febs.16127
27. Bradley LM, Douglass MF, Chatterjee D, Akira S, Baaten BJ. *Matrix metalloprotease 9 mediates neutrophil migration into the airways in response to influenza virus-induced toll-like receptor signaling. PLoS Pathog* 2012;**8**:e1002641. https://doi.org/10.1371/journal.ppat.1002641
28. Beigelman A, Goss CW, Wang J, Srinivasan M, Boomer J, Zhou Y, et al. *Azithromycin therapy in infants hospitalized for respiratory syncytial virus bronchiolitis: airway matrix metalloproteinase-9 levels and subsequent recurrent wheeze. Ann Allergy Asthma Immunol* 2024;**132**:623–9. https://doi.org/10.1016/j.anai.2024.01.001
29. Bai S, Wang W, Ye L, Fang L, Dong T, Zhang R, et al. *IL-17 stimulates neutrophils to release S100A8/A9 to promote lung epithelial cell apoptosis in Mycoplasma pneumoniae-induced pneumonia in children. Biomed Pharmacother* 2021;**143**:112184. https://doi.org/10.1016/j.biopha.2021.112184
30. Bengtsson AA, Sturfelt G, Lood C, Rönnblom L, van Vollenhoven RF, Axelsson B, et al. *Pharmacokinetics, tolerability, and preliminary efficacy of Paquinimod (ABR-215757), a new quinoline-3-carboxamide derivative: studies in lupus-prone mice and a multicenter, randomized, double-blind, placebo-controlled, repeat-dose, dose-ranging study in patients with systemic lupus erythematosus. Arthritis Rheum* 2012;**64**:1579–88. https://doi.org/10.1002/art.33493
31. Koch CM, Prigge AD, Setar L, Anekalla KR, Do-Umehara HC, Abdala-Valencia H, et al. *Cilia-related gene signature in the nasal mucosa correlates with disease severity and outcomes in critical respiratory syncytial virus bronchiolitis. Front Immunol* 2022;**13**:924792. https://doi.org/10.3389/fimmu.2022.924792
32. Zaas AK, Chen M, Varkey J, Veldman T, Hero 3rd AO, Lucas J, et al. *Gene expression signatures diagnose influenza and other symptomatic respiratory viral infections in humans. Cell Host Microbe* 2009;**6**:207–17. https://doi.org/10.1016/j.chom.2009.07.006
33. Ascough S, Dayananda P, Kalyan M, Kuong SU, Gardener Z, Bergstrom E, et al. *Divergent age-related humoral correlates of protection against respiratory syncytial virus infection in older and young adults: a pilot, controlled, human infection challenge model. Lancet Healthy Longev* 2022;**3**:e405–16. https://doi.org/10.1016/S2666-7568(22)00103-9
34. Groves HT, Cuthbertson L, James P, Moffat MF, Cox M, Tregoning JS. *Respiratory disease following viral lung infection alters the murine gut microbiota. Front Immunol* 2018;**9**:182. https://doi.org/10.3389/fimmu.2018.00182
35. Schenck LP, McGrath JJC, Lamarche D, Stämpfli MR, Bowdish DME, Surette MG. *Nasal tissue extraction is essential for characterization of the murine upper respiratory tract microbiota. mSphere* 2020;**5**:e00562-20. https://doi.org/10.1128/mSphere.00562-20
36. Harker JA, Lee DC, Yamaguchi Y, Wang B, Bukreyev A, Collins PL, et al. *Delivery of cytokines by recombinant virus in early life alters the immune response to adult lung infection. J Virol* 2010;**84**:5294–302. https://doi.org/10.1128/JVI.02503-09
37. Yamaguchi Y, Harker JA, Wang B, Openshaw PJ, Tregoning JS, Culley FJ. *Preexposure to CpG protects against the delayed effects of neonatal respiratory syncytial virus infection. J Virol* 2012;**86**:10456–61. https://doi.org/10.1128/JVI.01082-12
38. Bolger AM, Lohse M, Usadel B. *Trimmomatic: a flexible trimmer for Illumina sequence data. Bioinformatics* 2014;**30**:2114–20. https://doi.org/10.1093/bioinformatics/btu170
39. Liao Y, Smyth GK, Shi W. *featureCounts: an efficient general purpose program for assigning sequence reads to genomic features. Bioinformatics* 2014;**30**:923–30. https://doi.org/10.1093/bioinformatics/btt656
40. Wickham H. *From book elegant graphics for data analysis.* ggplot2: elegant graphics for data analysis. Springer-Verlag; 2009.
41. Ritchie ME, Phipson B, Wu D, Hu Y, Law CW, Shi W, et al. *limma powers differential expression analyses for RNA-sequencing and microarray studies. Nucleic Acids Res* 2015;**43**. https://doi.org/10.1093/nar/gkv007. e47-e47.
42. Wu T, Hu E, Xu S, Chen M, Guo P, Dai Z, et al. *clusterProfiler 4.0: a universal enrichment tool for interpreting omics data. Innovation* 2021;**2**:100141. https://doi.org/10.1016/j.xinn.2021.100141
43. Subramanian A, Tamayo P, Mootha VK, Mukherjee S, Ebert BL, Gillette MA, et al. *Gene set enrichment analysis: a knowledge-based approach for interpreting genome-wide expression profiles. Proc Natl Acad Sci USA* 2005;**102**:15545–50. https://doi.org/10.1073/pnas.0506580102
44. Zhou G, Soufan O, Ewald J, Hancock REW, Basu N, Xia J. *NetworkAnalyst 3.0: a visual analytics platform for comprehensive gene expression profiling and meta-analysis. Nucleic Acids Res* 2019;**47**:W234–41. https://doi.org/10.1093/nar/gkz240
45. Cheng X, Yan J, Liu Y, Wang J, Taubert S. *eVITTA: a web-based visualization and inference toolbox for transcriptome analysis. Nucleic Acids Res* 2021;**49**:W207–15. https://doi.org/10.1093/nar/gkab366
46. Habibi MS, Thwaites RS, Chang M, Jozwik A, Paras A, Kirsebom F, et al. *Neutrophilic inflammation in the respiratory mucosa predisposes to RSV infection. Science* 2020;**370**:eaba9301. https://doi.org/10.1126/science.aba9301